SCIENCE CHINA
Technological Sciences

•Article•

December 2020 Vol.63 No.12: 2606–2616
https://doi.org/10.1007/s11431-020-1721-6

Analytical solution to one-dimensional mathematical model of flow and morphological evolution in open channels

DING Yun[1,2], LI ZuiSen[3,4*], SHI YongZhong[3,4] & ZHONG DeYu[5,6*]

[1] *State Key Laboratory of Hydrology-Water Resources and Hydraulic Engineering, Hohai University, Nanjing 210098, China;*
[2] *College of Water Conservancy and Hydropower Engineering, Hohai University, Nanjing 210098, China;*
[3] *Zhejiang Institute of Hydraulics and Estuary, Hangzhou 310008, China;*
[4] *Zhejiang Provincial Key Laboratory of Hydraulic Disaster Prevention and Mitigation, Hangzhou 310008, China;*
[5] *Joint-Sponsored State Key Laboratory of Plateau Ecology and Agriculture, Qinghai University, Xining 810016, China;*
[6] *State Key Laboratory of Hydroscience and Engineering, Tsinghua University, Beijing 100084, China*

Received July 27, 2020; accepted September 7, 2020; published online October 23, 2020

The evolution of open-channel flow and morphology can be simulated by one-dimensional (1D) mathematical models. These models are typically solved by numerical or analytical methods. Because the behavior of variables can be explained by explicit mathematical determinations, compared to numerical solutions, analytical solutions provide fundamental and physical insights into flow and sediment transport mechanisms. The singular perturbation technique derives a hierarchical equation of waves and describes the evolutionary nature of disturbances in hyperbolic systems. The wave hierarchy consists of dynamic, diffusion, and kinetic waves. These three types of waves interact with each other in the process of propagation. Moreover, the Laplace transform is implemented to transform partial differential equations into ordinary differential equations. Analytical expressions in the wave front are subtracted by the approximation of kinetic and diffusion models. Moreover, an analytical solution consists of a linear combination of the kinetic wave front and the diffusion wave front expressions, pursuing to describe the physical mechanism of motion in open channels as completely as possible. Analytical solutions are presented as a combination of exponential functions, hyperbolic functions, and infinite series. The obtained analytical solution was further applied to the simulation of flood path and morphological evolution in the Lower Yellow River. The phenomenon of increased peak discharge in the downstream reach was successfully simulated. It was encouraging that the results were in good agreement with the observed data.

open channel, mathematical model, analytical solution, Laplace transform, morphological evolution

Citation: Ding Y, Li Z S, Shi Y Z, et al. Analytical solution to one-dimensional mathematical model of flow and morphological evolution in open channels. Sci China Tech Sci, 2020, 63: 2606–2616, https://doi.org/10.1007/s11431-020-1721-6

1 Introduction

Understanding the flow mechanism and morphological evolution is crucial for river training, flood control, water resources management, and environmental improvements. Physically, the flow and sedimentation processes as well as morphological evolution are inconsistent on temporal and spatial scales. Moreover, climate change and human intervention have exacerbated the inconsistencies in recent decades. For instance, highly nonequilibrium sediment transport due to extreme flooding and watershed erosion further complicates the evolution of flow hydrodynamics and river morphology [1,2].

One-dimensional mathematical models have been widely developed in simulating open-channel flow and morphological evolution. The reader may be familiar with some very

*Corresponding authors (email: lizuisen@hotmail.com; zhongdy@tsinghua.edu.cn)

famous models, such as Mike11 [3] and HEC-6 [4]. A detailed review of 1D mathematical models is available in the literature [5–12]. In many practical cases where the capacity of sediment transport is low, and the morphology changes on a long-term scale, 1D models provide considerable satisfaction, considering the easy setup and calibration efficiency. Nevertheless, the application of 1D models has been less successful for local alluvial processes such as rapid and significant riverbed aggradation or degradation. Many researchers have endeavored to address the deficiencies [13–17]. Studies generally fall into two aspects: (1) physical background and (2) solutions. In terms of physical background, the governing equations for 1D models are derived based on a series of assumptions. The shallow-water equations are based on the fixed bed assumption. In this case, the evolution rate of riverbed morphology is considered to be a relatively low order of magnitude flow with low sediment concentrations. Therefore, flow bed mobility is not considered in the flow continuity equation.

In contrast, the spatial gradient of sediment concentration and temporal momentum transfer between sediment-laden flows and erodible riverbeds are mostly ignored in the flow-momentum equations [13–17]. In addition, sediment transport and bed deformation equations are mainly based on the dynamic wave models [18–21] or diffusion wave models [18,22]. Sediment transport capacity is expressed by the relationship between the flow rate variables and sediment flux. Then, an equilibrium condition between aggradation and degradation rate is assumed.

One-dimensional models are typically solved by numerical or analytical methods. Numerous numerical schemes and algorithms have been developed to solve the equations efficiently [23–26]. Most recently, several modern computational schemes have been proposed, which can be conveniently applied to multidimensional physical problems with complex properties [27–32]. Compared to numerical methods, analytical solutions are extensively implemented and provide much important information about the complex evolution of dynamic systems [33–38]. Because the flow behavior, sedimentation, and morphology in open channels can be explained by explicit mathematical determinations related to specified initial and boundary conditions, the analytical solution of a hydrodynamic model provides fundamental and physical insights into the mechanism of flow and morphological evolution [34,35]. In addition, the analytical solution can provide a benchmark for numerical algorithms.

In general, it is difficult to derive analytical solutions for 1D mathematical models of flow and morphological evolution due to the robust nonlinear systems that the model builds. Some researchers have simplified and linearized the equations governing wave approximation [39–45]. Integral transform techniques are implemented to transform partial differential equations into ordinary differential equations to formulate analytical expressions [45,46]. The approximation of the Saint–Venant equation, called the dynamic wave model, allows other simplified wave models, such as kinematic wave [42,43], gravitational wave [41], noninertial wave [42], and quasi-steady dynamic wave [42,46] models, to be widely used in open-channel flows under certain circumstances. Furthermore, Hayami [47] established an analytical solution for the diffusion wave model of channel flows, considering upstream boundary conditions. The diffusion wave model is developed by ignoring the local acceleration and convection acceleration terms. The solution applies to different patterns of friction laws and cross-section shapes. Following Hayami [47], Tingsanchali and Manandhar [48] developed an analytical diffusion model for flood routing that considers backwater effects and lateral flows. Tsai [42] obtained analytical solutions for kinetic wave, noninertia wave, gravity wave, and quasi-steady dynamic wave models of shallow-water waves in open channels. The analysis emphasized on downstream boundary condition feedback. Kazezyılmaz-Alhan and Medina [34] derived an analytical solution for diffusion waves with constant wave velocity and hydraulic diffusivity in overland flows.

The purpose of this study is to obtain an analytical solution for a 1D mathematical model of flow and morphological evolution in open channels. The literature review indicates that most of the research to date has solely focused on the propagation of water waves. It is necessary to emphasize that the analytical description for flow, sediment, and morphological evolution provided in the present study was first reported. Moreover, unlike in previous studies, complete governing equations that incorporate the interaction between flow and sediment transport have been adopted to make representative models further. The set of governing equations is linearized, and a singular perturbation technique is implemented. A hierarchical equation of waves is derived that can characterize the disturbance evolution in a quasi-steady hyperbolic system. The Laplace transform is used to subtract the analytical expression of flow, sediment, and morphological evolution. Analytical solutions in the literature are mainly conducted on separate kinetic or diffusion wave models. This study linearly combines kinetic and diffusive wave front analytical expressions to address interactions in wave hierarchy and avoid potential deviations in simplification. The analytical expressions obtained are further applied in practical situations. The present work can provide an insightful approach to study the hydrodynamics of open-channel flows and improve the accuracy of mathematical modeling.

2 Mathematical model

For a hydraulically wide rectangular open channel with a

constant width and an erodible bed composed of uniform sediment particles, the governing equations for the 1D mathematical model are [13,17]

$$\frac{\partial h(1-s)}{\partial t}+\frac{\partial hu(1-s)}{\partial x}+p\frac{\partial \Delta z}{\partial t}=0, \tag{1}$$

$$\underset{\text{(a)}}{\frac{\partial u}{\partial t}}+\underset{\text{(b)}}{u\frac{\partial u}{\partial x}}+\underset{\text{(c)}}{g\frac{\partial (h+\Delta z)}{\partial x}}+\underset{\text{(d)}}{\frac{(\rho_s-\rho_w)gh}{2\rho_m}\frac{\partial s}{\partial x}}$$

$$\underset{\text{(e)}}{-\frac{u\rho_b}{h\rho_m}\frac{\partial \Delta z}{\partial t}}=\underset{\text{(f)}}{g}\underset{\text{(g)}}{\left(i_0-i_f\right)}, \tag{2}$$

$$\frac{\partial hs}{\partial t}+\frac{\partial hus}{\partial x}=\alpha_s\omega_s(s_{eq}-s), \tag{3}$$

$$\frac{\partial \Delta z}{\partial t}=-\frac{\alpha_s\omega_s(s_{eq}-s)}{1-p}, \tag{4}$$

where h=flow depth; u=mean velocity of flow; s=volumetric suspended sediment concentration; Δz=vertical variation of bed elevation; p=bed sediment porosity; i_0=bed slope; i_f=friction slope; s_{eq}=volumetric equilibrium suspended sediment concentration; ρ_w and ρ_w=density of sediment and clear water, respectively; ρ_m=density of a flow-sediment mixture, $\rho_m=(1-s)\rho_w+s\rho_s$; ρ_b=density of saturated bed material, $\rho_b=p\rho_w+(1-p)\rho_s$; α_s=nonequilibrium adaptation coefficient of suspended load; ω_s=settling velocity of single sediment; g=gravity acceleration; t and x=independent variables of time and streamwise coordinate, respectively.

Eq. (1) is the modified version of the Saint–Venant continuity equation that incorporates sediment concentration and riverbed deformation [13,17]. Eq. (2) is the modified Saint–Venant momentum equation. The term (d) in eq. (2) denotes the longitudinal gradient of suspended sediment concentration, and the term (e) represents the momentum exchange between the sediment-laden flow and the riverbed [13, 17]. In the context of alluvial processes with low sediment transport rate and weak bed deformation, terms (d) and (e) in eq. (2) are usually omitted. The parameters s and Δz in eq. (1) are treated as zero. Hence, eqs. (1) and (2) are simplified to the traditional Saint–Venant equation. The importance and need for incorporating sediment transport and bed deformation feedback into the shallow-water equation can be found in the literature [13–17]. In this study, eqs. (1) and (2) were adopted to make the model more representative.

Eqs. (3) and (4) are the nonequilibrium transport equations for suspended load in the sediment-laden flow and movable riverbed, respectively. The term ($s_{eq}-s$) on the right side of eqs. (3) and (4) denotes the detachment rate ($s_{eq}>s$) or the deposition rate ($s_{eq}<s$).

There are still some parameters that need to be determined to close the model. In open-channel flows, the friction slope can be calculated by Manning's formula $i_f=n_s^2u^2/h^{-4/3}$, Chezy's formula $i_f=u^2/hC_z^2$, or Darcy-Weisbach's formula $i_f=f_Du^2/(8gh)$, where n_s is the Manning coefficient, C_z is the Chezy coefficient, and f_D is the Darcy-Weisbach coefficient [42]. The Chezy coefficient C_z varies with flow depth, and the Darcy-Weisbach coefficient f_D is a function of Reynolds number and flow roughness. The Manning coefficient n is considered to be constant in a fully developed turbulent flow [46]. To avoid complex calculations, Manning's formula is used in this study.

The equilibrium suspended sediment concentration is calculated as $s_{eq}=k_s\left[uJ_w/\left(gh\omega_s\right)\right]^{m_s}$, where k_s and m_s are two empirical parameters, k_s=0.452 and m_s=0.762, and J_w is the hydraulic slope [49].

The nonequilibrium adaptation coefficient of the suspended load α_s in eqs. (3) and (4) is the ratio of near-bed sediment concentration to depth-averaged sediment concentration. α_s varies from 0.001 for deposition to 1.0 for erosion [9]. In addition, the settling velocity of sediment ω_s is expressed as $\omega_s=\omega_0(1-1.25s)\left[1+s/\left(2.25\sqrt{\overline{d}}\right)\right]^{3.5}$ [9], in which ω_s is the sediment settling velocity in clear water and $\overline{d}$ is the median diameter of bed material.

3 Wave hierarchy of 1D mathematical model

Eqs. (1)–(4) mathematically constitute a nonlinear hyperbolic system whose analytical solution is very difficult to obtain without approximation [34,46]. Flood propagation and nonequilibrium sediment transport in open channels can demonstrate the evolution of disturbances applied to uniform flows in equilibrium [46,50]. Hence, eqs. (1)–(4) are linearized into a quasi-steady hyperbolic system. As a result, a wave hierarchy dynamic equation can be constructed.

3.1 Wave hierarchy equation

To nondimensionalize eqs. (1)–(4), the scaling variables are introduced as follows:

$$u=U_0u',h=H_0h',\Delta z=H_0\xi',\\ s=s_{eq0}s',J_w=J_{w0}J'_w, \tag{5}$$

where U_0, H_0, s_{eq0}, and J_{w0} denote the characteristic scales for flow velocity, flow depth, equilibrium sediment concentration, and hydraulic slope, respectively. In addition, a typical horizontal length L_0 is introduced as a uniform flow drop at depth H_0, $x=L_0x'$, and $t=(L_0/U_0)t'$.

For open-channel flows, disturbances applied to a uniform flow with equilibrated sediment transport can be expressed as [46,50,51]

$$u'=1+\varepsilon^*u^*,h'=1+\varepsilon^*h^*,J'_w=1+\varepsilon^*J_w^*,\\ s'=1+\varepsilon^*s^*,\xi'=\varepsilon^*\xi^*, \tag{6}$$

where ε^* denotes the magnitude of the disturbance; u^*, h^*, J_w^*,

s^*, and ξ^* are the perturbed quantities of magnitude $O(1)$.

Substituting the relationships in eqs. (5) and (6) into eqs. (1)–(4) and slightly algebraic manipulation, we obtain the following quasi-steady hyperbolic system of equations governing the perturbed quantities:

$$\frac{\partial h^*}{\partial t}+\frac{\partial u^*}{\partial x}+\frac{\partial h^*}{\partial x}+\frac{\partial \xi^*}{\partial t}=0, \tag{7}$$

$$\frac{\partial u^*}{\partial t}+\frac{\partial u^*}{\partial x}+\frac{1}{\mathbf{F}_0^2}\frac{\partial h^*}{\partial x}+\frac{1}{\mathbf{F}_0^2}\frac{\partial \xi^*}{\partial x}+\frac{\alpha}{\mathbf{F}_0^2}\frac{\partial s^*}{\partial x}-\beta\frac{\partial \xi^*}{\partial t}=\sigma\left(\frac{4}{3}h^*-2u^*\right), \tag{8}$$

$$\frac{\partial s^*}{\partial t}+\frac{\partial s^*}{\partial x}+\delta\frac{\partial \xi^*}{\partial t}=0, \tag{9}$$

$$\frac{\partial \xi^*}{\partial t}=\mu\cdot\left(s^*-m_s u^*\right), \tag{10}$$

where $\alpha=\frac{s_{eq0}(\rho_s-\rho_w)}{2\left[s_{eq0}(\rho_s-\rho_w)+\rho_w\right]}$, $\beta=\frac{2\alpha}{s_{eq0}}$, $\sigma=\frac{gn^2L_0}{H_0^{4/3}}$, $\delta=\frac{1-p}{s_{eq0}}-1$, $\mu=\frac{\alpha\omega L_0 s_{eq0}}{(1-p)H_0}$, $\mathbf{F}_0=U_0/\sqrt{gH_0}$ is the uniform flow Froude number with equilibrium sediment transport.

The wave hierarchy equation in eqs. (7)–(10) can be derived using eqs. (8)–(10) after eliminating h^*, u^*, and s^* from eq. (7). The detailed procedure for algebraic manipulation is given in the Appendix. The factorized form of the wave hierarchy in eqs. (7)–(10) is

$$-\frac{1}{m_s\mu}\prod_{i=1}^{4}\left(\frac{\partial}{\partial t}+\lambda_i\frac{\partial}{\partial x}\right)\xi^*-\left(\beta+\frac{\delta}{m_s}+\frac{2\sigma}{m_s\mu}\right)\prod_{i=1}^{3}\left(\frac{\partial}{\partial t}+C_i\frac{\partial}{\partial x}\right)\xi^*+\left(\frac{4}{3}\sigma-\frac{2\sigma\delta}{m_s}\right)\prod_{i=1}^{2}\left(\frac{\partial}{\partial t}+a_i\frac{\partial}{\partial x}\right)\xi^*=0, \tag{11}$$

where λ_i (i=1, 2, 3, 4) satisfies the function

$$\psi(\lambda)=\lambda^4-3\lambda^3+\frac{3\mathbf{F}_0^2-1}{\mathbf{F}_0^2}\lambda^2-\frac{\mathbf{F}_0^2-1}{\mathbf{F}_0^2}\lambda. \tag{12}$$

C_i (i=1, 2, 3) corresponds to three real zeros of a cubic function,

$$\psi(C)=C^3-\frac{\left(\frac{2\delta}{m_s}+\mathbf{F}_0^{-2}\alpha\delta+2\beta+\frac{16\sigma}{3m_s\mu}\right)}{\beta+\frac{\delta}{m_s}+\frac{2\sigma}{m_s\mu}}C^2-\frac{\left(\mathbf{F}_0^{-2}-\mathbf{F}_0^{-2}\alpha\delta-\beta-\frac{10\sigma}{3m_s\mu}-\frac{\left(1-\mathbf{F}_0^{-2}\right)\delta}{m_s}\right)}{\beta+\frac{\delta}{m_s}+\frac{2\sigma}{m_s\mu}}C+\frac{\mathbf{F}_0^{-2}}{\beta+\frac{\delta}{m_s}+\frac{2\sigma}{m_s\mu}}, \tag{13}$$

and for a_i (i=1, 2),

$$a_1=\left(\frac{4}{3}-\frac{10\delta}{3m_s}\right)/\left(\frac{4}{3}-\frac{2\delta}{m_s}\right), a_2=0. \tag{14}$$

The quasi-steady hyperbolic system that governs the flow and sediment transport under nonequilibrium conditions in open channels is reduced to the wave hierarchy eq. (11). Needham [50] constructed a wave hierarchy equation for bed-load transport under equilibrium conditions:

$$\frac{U_0}{2gJ_{w0}T_0}(1+\varepsilon)\prod_{i=1}^{3}\left(\frac{\partial}{\partial t}+C_i\frac{\partial}{\partial x}\right)\xi^*+\prod_{i=1}^{2}\left(\frac{\partial}{\partial t}+a_i\frac{\partial}{\partial x}\right)\xi^*=0, \tag{15}$$

where ε measures the effect of bed-load sediment transport on flow resistance.

3.2 Properties of wave hierarchy

A consideration of eq. (11) indicates that the wave hierarchy consists of three types of waves with different energy magnitude. The higher fourth-order wave λ is denoted as a dynamic wave, the lower second-order wave a has the property of a kinetic wave, and the "middle" third-order wave C is recognized as a diffusion wave in this study. A physical understanding of wave hierarchy can be shown as disturbances (i.e., variations of flow and sediment conditions within boundaries) applied to a uniform flow with equilibrium sediment transport in open channels carried by dynamic, diffusion, and kinetic waves. The propagation characteristics of these waves are different from each other. Moreover, these three types of waves interact with each other during evolution [51].

The four real zeros of the function in eq. (12) are $\lambda_1=1-\mathbf{F}_0^{-1}$, λ_2=0, λ_3=1, and $\lambda_4=1+\mathbf{F}_0^{-1}$, where λ_1 and λ_2 are analogous to traditional dynamic waves of fixed bed hydraulics [7,51]. λ_2 and λ_3 are the bedform wave and sediment wave, respectively. Figure 1 shows variations of λ. It is observed that λ only depend on $\mathbf{F}_0$ but is independent of the coupling of sediment transport and river mobility. In subcritical flows, the sequence of the dynamic wave speed is $\lambda_1<0<\lambda_3<\lambda_4$. In contrast, the sequence is $0<\lambda_1<\lambda_3<\lambda_4$ in supercritical flows.

Because the coefficients in eq. (13) are complex, the asymptotic polynomial approximation can be used to solve the three roots of the cubic function in eq. (13). The sequence of the diffusion wave speed is $C_1<0<C_2<C_3$. Research on the "mysterious" diffusion wave is rarely found in the literature. It is tempting to infer that the diffusion wave C plays a non-negligible role in the evolution of the imposed disturbances. It may determine the accuracy of predictions. A consideration of eq. (13) demonstrates that C is not only dependent on F_0 but also on flow friction and equilibrium sediment concentration. Figure 2 shows variations in C with different s_{eq0}

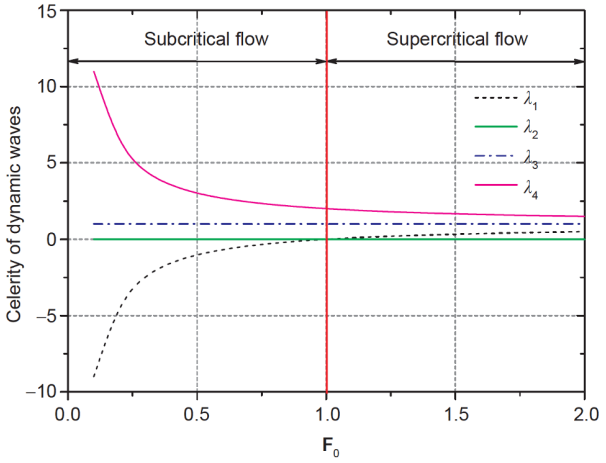

Figure 1 (Color online) Speed variation of dynamic waves with Froude number.

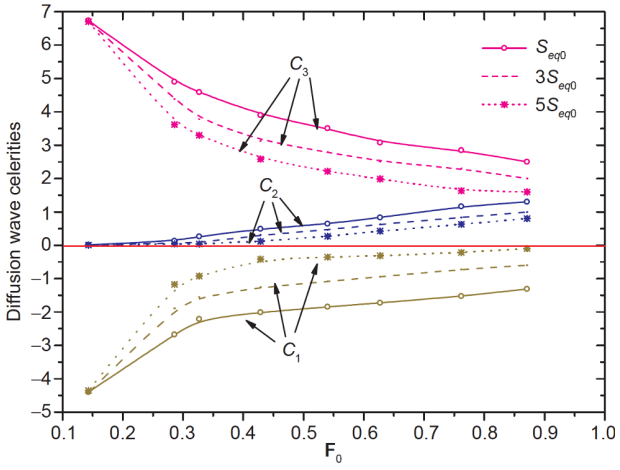

Figure 2 (Color online) Speed variation of diffusion waves with Froude number.

values. This indicates that sediment concentration "slows down" the propagation of diffusion wave C.

For the kinetic waves a_i (i=1, 2), an observation from eq. (14) indicates that a_2 is a diffusive bedform wave, and a_1 is analogous to a "flood wave". It is necessary to note that if the terms (d) and (e) are omitted in eq. (2), a_1 is reduced to 5/3. This is the kinetic wave speed in fixed bed hydraulics. As shown in Figure 3, the propagation of the kinetic wave a_1 is affected by equilibrium sediment concentration in a uniform flow. The higher the s_{eq0}, the faster the a_1 propagates.

4 Analytical solution

Compared to numerical methods, analytical solutions for linearized mathematical models provide fundamental and physical insights into flow mechanisms and morphological evolution in open channels [46]. The Laplace transform is effectively implemented to formulate analytical expressions [45,46,48].

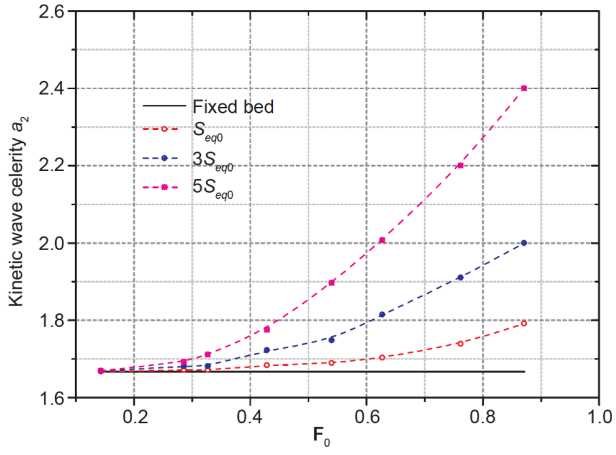

Figure 3 (Color online) Speed variation of kinetic waves with Froude number.

4.1 Kinetic wave front expansion

Following Whitham [51], a simplified treatment named wave front expansion is defined as

$$\frac{\partial}{\partial t} \simeq -V\frac{\partial}{\partial x}, \tag{16}$$

where V denotes the wave front.

By using eq. (16) in eqs. (7)–(10), the partial derivative of time is replaced by a spatial derivative along the characteristic line of kinetic wave propagation in a quasi-steady hyperbolic system. Then we can obtain

$$\begin{aligned} s^* &= \frac{V\delta}{(1-V)}\xi^*, u^* = \frac{V\delta}{(1-V)m_s}\xi^* + \frac{V}{m_s\mu}\frac{\partial\xi^*}{\partial x}, \\ h^* &= \frac{V}{1-V}\left[1-\frac{\delta}{(1-V)m_s}\right]\xi^* - \frac{V}{(1-V)m_s\mu}\frac{\partial\xi^*}{\partial x}. \end{aligned} \tag{17}$$

A consideration of eq. (17) indicates that the perturbed quantities u^*, h^*, and s^* are expressed as a function of ξ^*. Once the analytical expression of ξ^* is established, a complete analytical solution for eqs. (7)–(10) can be obtained. Substituting expressions of eq. (17) into eq. (11) with some algebraic manipulation, the wave hierarchy developed in the kinetic wave front arrives at

$$\frac{\partial\xi^*}{\partial t} + a_i\frac{\partial\xi^*}{\partial x} = \tau_i\frac{\partial^2\xi^*}{\partial x^2} + \upsilon_i\frac{\partial^3\xi^*}{\partial x^3}, \tag{18}$$

where

$$\tau_i = -\frac{\left(\beta + \frac{\delta}{m_s} + \frac{2\sigma}{m_s\mu}\right)\psi(a_i)}{\left(\frac{4}{3}\sigma - \frac{2\sigma\delta}{m_s}\right)\prod_{\substack{j=1 \\ j\neq i}}^{2}(a_j - a_i)},$$

$$\upsilon_i = \frac{(\lambda_1 - a_i)(\lambda_2 - a_i)(\lambda_3 - a_i)(\lambda_4 - a_i)}{m_s\mu\left(\frac{4}{3}\sigma - \frac{2\sigma\delta}{m_s}\right)\prod_{\substack{j=1 \\ j\neq i}}^{2}(a_j - a_i)}.$$

Eq. (18) is a type of convection-diffusion equation. The left side of eq. (18) denotes that the kinetic wave dominates

the convection of morphological evolution. Moreover, the source terms on the right side of eq. (18) address the diffusion in morphological evolution. An observation of coefficients τ_i and υ_i denotes that the diffusion wave propagation C_i and interactions between dynamic waves λ_i and kinetic waves a_i affect the diffusion characteristics. In the situation of a kinetic wave propagating downstream (a_2>0), there exist τ_2>0 and υ_2>0. This means that the kinetic wave is attenuated by the dissipation of the source [51,52].

4.2 Laplace transform

The following integral defines the Laplace transform of ξ^*:

$$Z(x,\mathrm{p}) = \mathbf{L}\{\xi^*(x,t)\} = \int_0^\infty \xi^*(x,t)\mathrm{e}^{-t\mathrm{P}}\mathrm{d}t, \tag{19}$$

where Z is the transformed ξ^* and P is a complex variable.

To avoid mathematical difficulties, the second term on the right side of eq. (18) is omitted in the process of deriving the analytical expression, given that the third derivative plays a relatively weak role in dissipation. Implementing eq. (19) into eq. (18), the ordinary differential equation (ODE) of the transformed domain is

$$\frac{\mathrm{d}^2 Z}{\mathrm{d}x^2} - \frac{a_i}{\tau_i}\frac{\mathrm{d}Z}{\mathrm{d}x} - \frac{\mathrm{p}}{\tau_i}Z = 0. \tag{20}$$

The transformed initial and boundary conditions for eq. (18) are expressed as

$$Z(x,0) = 0, Z(0,\mathrm{p}) = \frac{f_\mathrm{u}(\mathrm{p})}{\mathrm{p}}, Z(1,\mathrm{p}) = 0, \tag{21}$$

where f_u(p) denotes the upstream boundary condition.

The general solution for eq. (20) in the transformed domain can be derived as

$$Z(x,\mathrm{p}) = \frac{f_\mathrm{u}(\mathrm{p})}{\mathrm{p}}\exp\left(\frac{a_i}{2\tau_i}x\right)\frac{\sinh\left[\tau_i^{-0.5}w'(1-x)\right]}{\sinh\left[\tau_i^{-0.5}w'\right]}, \tag{22}$$

where $w' = \left(a_i^{\,2}/(4\tau_i) + \mathrm{p}\right)^{0.5}$.

The inverse Laplace transform is

$$\xi^*(x,t) = \mathbf{L}^{-1}\{Z(x,\mathrm{p})\} = \frac{1}{2\pi\mathrm{i}}\int_{\sigma-\mathrm{i}\infty}^{\sigma+\mathrm{i}\infty} Z(x,\mathrm{p})\mathrm{e}^{t\mathrm{p}}\mathrm{d}\mathrm{p}. \tag{23}$$

Considering the relationship in Laplace transform [52]

$$\mathbf{L}^{-1}\{Z(x,\mathrm{p}+b)\} = \exp(-bt)\mathbf{L}^{-1}\{Z(x,\mathrm{p})\}, \tag{24}$$

where $b = a_i^{\,2}/(4\tau_i)$.

By using eq. (24), eq. (23) can be further expressed as

$$\begin{aligned}\xi^*(x,t) &= f_\mathrm{u}(t)\exp\left(\frac{a_i}{2\tau_i}x - bt\right)\\ &\cdot\mathbf{L}^{-1}\left\{\frac{\sinh\left[\tau_i^{-0.5}\mathrm{p}^{0.5}(1-x)\right]}{(\mathrm{p}-b)\sinh\left[\tau_i^{-0.5}\mathrm{p}^{0.5}\right]}\right\},\end{aligned} \tag{25}$$

where p=b, and $\mathrm{p}_n = -n^2\pi^2\tau_i$ (n=1, 2, 3…) are two singularities.

Based on the residue theorem for complex variable functions [53], the residues in eq. (25) can be calculated by

$$\begin{aligned}&\mathbf{L}^{-1}\left\{\frac{\sinh\left[\tau_i^{-0.5}\mathrm{p}^{0.5}(1-x)\right]}{(\mathrm{p}-b)\sinh\left[\tau_i^{-0.5}\mathrm{p}^{0.5}\right]}\right\} =\\ &\sum_n\left[\frac{\sinh\left[\tau_i^{-0.5}p^{0.5}(1-x)\right]\exp(\mathrm{p}_n t)}{\dfrac{\mathrm{d}(\mathrm{p}-b)\sinh\left[\tau_i^{-0.5}\mathrm{p}^{0.5}\right]}{\mathrm{d}\mathrm{p}}}\right]_{\mathrm{p}=\mathrm{p}_n}.\end{aligned} \tag{26}$$

The expanded form of Fourier sine series is

$$\frac{\sinh[\theta(1-x)]}{\sinh(\theta)} = 2\pi\sum_{n=1}^{\infty}\frac{n\sin(n\pi x)}{(\theta^2+n^2\pi^2)}, x \neq 0. \tag{27}$$

Finally, the analytical solution for eq. (18) is

$$\xi_{a_i}^*(x,t) = f_\mathrm{u}(t)\exp\left(\frac{a_i}{2\tau_i}x\right)\left\{\frac{\sinh\left[\tau_i^{-0.5}\dfrac{a_i}{2\tau_i}(1-x)\right]}{\sinh\left(\tau_i^{-0.5}\dfrac{a_i}{2\tau_i}\right)} - 2\pi\tau_i\sum_{n=1}^{\infty}\frac{n\sin(n\pi x)}{\left(\left(\dfrac{a_i}{2\tau_i}\right)^2 + n^2\pi^2\tau_i\right)}\exp\left[-\left(\left(\frac{a_i}{2\tau_i}\right)^2 + n^2\pi^2\tau_i\right)t\right]\right\}. \tag{28}$$

The analytical expression in eq. (28) consists of an exponential function, hyperbolic function, and infinite series. The calculation is mathematically feasible. Considering the relationships in eq. (17), analytical expressions of h^*, u^*, and s^* for the kinetic wave front can be written as

$$\begin{cases} h^*(x,t) = \dfrac{a_i}{1-a_i}\left[1 - \dfrac{\delta}{(1-a_i)m_\mathrm{s}}\right]\xi_{a_i}^*(x,t) - \dfrac{a_i}{(1-a_i)m_\mathrm{s}\mu}\dfrac{\partial\xi_{a_i}^*(x,t)}{\partial x}, \\ u^*(x,t) = \dfrac{a_i\delta}{(1-a_i)m_\mathrm{s}}\xi_{a_i}^*(x,t) + \dfrac{a_i}{m_\mathrm{s}\mu}\dfrac{\partial\xi_{a_i}^*(x,t)}{\partial x}, \\ s^*(x,t) = \dfrac{a_i\delta}{(1-a_i)}\xi_{a_i}^*(x,t). \end{cases} \tag{29}$$

4.3 Diffusion wave front expansion

The wave hierarchy in eq. (11) can be expanded for the diffusion wave as follows:

$$\frac{\partial \xi^*}{\partial t} + C_i \frac{\partial \xi^*}{\partial x} = \kappa_i \xi^* + \iota_i \frac{\partial^2 \xi^*}{\partial x^2}, \tag{30}$$

where

$$\kappa_i = \frac{\left(\frac{4}{3}\sigma - \frac{2\sigma\delta}{m_s}\right)(a_1 - C_i)(a_2 - C_i)}{\left(\beta + \frac{\delta}{m_s} + \frac{2\sigma}{m_s\mu}\right)\prod_{\substack{j=1 \\ j\neq i}}^{3}(C_j - C_i)},$$

$$\iota_i = -\frac{(\lambda_1 - C_i)(\lambda_2 - C_i)(\lambda_3 - C_i)(\lambda_4 - C_i)}{m_s\mu\left(\beta + \frac{\delta}{m_s} + \frac{2\sigma}{m_s\mu}\right)\prod_{\substack{j=1 \\ j\neq i}}^{3}(C_j - C_i)}.$$

The left side of eq. (30) denotes that the diffusion wave dominates the convection of morphological evolution. If the second term on the right side of eq. (30) is ignored, then eq. (30) is transformed into a non-homogeneous convection equation, and its solution is

$$\xi^*{}_{C_i}(x,t) = \exp(\kappa_i t) G(x - C_i t), \tag{31}$$

where G is a function of $x - C_i t$ and can be specified by the initial and boundary conditions.

Analytical expressions of h^*, u^*, and s^* for the diffusion wave front are written as

$$\begin{cases} h^*(x,t) = \dfrac{C_i}{1-C_i}\left[1 - \dfrac{\delta}{(1-C_i)m_s}\right]\exp(\kappa_i t)G(x - C_i t) \\ \qquad\qquad - \dfrac{C_i}{(1-C_i)m_s\mu}\exp(\kappa_i t)\dfrac{\partial G(x - C_i t)}{\partial x}, \\ u^*(x,t) = \dfrac{C_i\delta}{(1-C_i)m_s}\exp(\kappa_i t)G(x - C_i t) \\ \qquad\qquad + \dfrac{C_i}{m_s\mu}\exp(\kappa_i t)\dfrac{\partial G(x - C_i t)}{\partial x}, \\ s^*(x,t) \simeq \dfrac{C_i\delta}{(1-C_i)}\exp(\kappa_i t)G(x - C_i t). \end{cases} \tag{32}$$

Tsai and Yen [46], Kazezyılmaz-Alhan and Medina [34] established analytical solutions for the diffusion wave model. As shown in eq. (32), the solution expressions they obtained were a similar form of an exponential function.

4.4 Analytical expressions

As aforementioned discussed, the kinetic wave and diffusion wave approximations are widely used in the modeling of open channel hydraulic flows. The kinetic wave approximation is appropriate for a channel with a moderate slope and weak backwater from downstream. However, it cannot account for the gradually varying flow condition as the disperse term is neglected [39]. The diffusion wave approximation is applicable in channels with slopes ranging from 0.001 to 0.0001, and it introduces the physical diffusion [7]. Moreover, analytical solutions in the literature are mostly conducted to separate kinetic wave or diffusion wave models. To consider the interactions in the wave hierarchy and to avoid the potential lack of simplification, this study makes a linear combination of the analytical expressions in the kinetic wave front together with those in the diffusion wave front. It is necessary to note that, if the kinetic wave or diffusion wave model was initially adopted as the mathematical model, as most of the studies in the literature did, it is impossible to illustrate the interactions between waves of the different magnitude of energy or to describe the physical mechanism of motion in the open channel as complete as possible. Thus, the analytical solution to the 1D mathematical model of flow and morphological evolution is given as

$$\begin{cases} h^*(x,t) = \dfrac{a_i}{1-a_i}\left[1 - \dfrac{\delta}{(1-a_i)m_s}\right]\xi^*_{a_i}(x,t) \\ \qquad\qquad - \dfrac{a_i}{(1-a_i)m_s\mu}\dfrac{\partial \xi^*_{a_i}(x,t)}{\partial x} \\ \qquad\qquad + \dfrac{C_i}{1-C_i}\left[1 - \dfrac{\delta}{(1-C_i)m_s}\right]\exp(\kappa_i t)G(x - C_i t) \\ \qquad\qquad - \dfrac{C_i}{(1-C_i)m_s\mu}\exp(\kappa_i t)\dfrac{\partial G(x - C_i t)}{\partial x}, \\ u^*(x,t) = \dfrac{a_i\delta}{(1-a_i)m_s}\xi^*_{a_i}(x,t) + \dfrac{a_i}{m_s\mu}\dfrac{\partial \xi^*_{a_i}(x,t)}{\partial x} \\ \qquad\qquad + \dfrac{C_i\delta}{(1-C_i)m_s}\exp(\kappa_i t)G(x - C_i t) \\ \qquad\qquad + \dfrac{C_i}{m_s\mu}\exp(\kappa_i t)\dfrac{\partial G(x - C_i t)}{\partial x}, \\ s^*(x,t) = \dfrac{a_i\delta}{(1-a_i)}\xi^*_{a_i}(x,t) + \dfrac{C_i\delta}{(1-C_i)}\exp(\kappa_i t)G(x - C_i t), \\ \xi^*(x,t) = \xi^*_{a_i}(x,t) + \exp(\kappa_i t)G(x - C_i t). \end{cases} \tag{33}$$

5 Applications

The analytical solutions of eqs. (33) and (28) were applied in August 1992 in the Lower Yellow River region of China by simulating flood path with hyperconcentrated sediment transport [54]. As shown in Figure 4, the channel length L_0 considered is approximately 150 km from Xiaolangdi Gauge Station to Huanyuankou Gauge Station. The average bed slope J_{w0} is 0.12‰. The Manning coefficient n_s is 0.015. Figure 5 shows the upstream boundary conditions of flood discharge and sediment concentration of the 1992 flood event. The flood route of Xiaolangdi Station can be roughly divided into two stages. The first stage flood peak was 3000 $m^3\ s^{-1}$, and the sediment concentration in the water body was relatively low. A few days later, a second stage flood route with a peak of 4570 $m^3\ s^{-1}$ occurred shortly after the first stage. The sediment concentration in the second stage rose sharply to over 535 $kg\ m^{-3}$. Flood routes of the

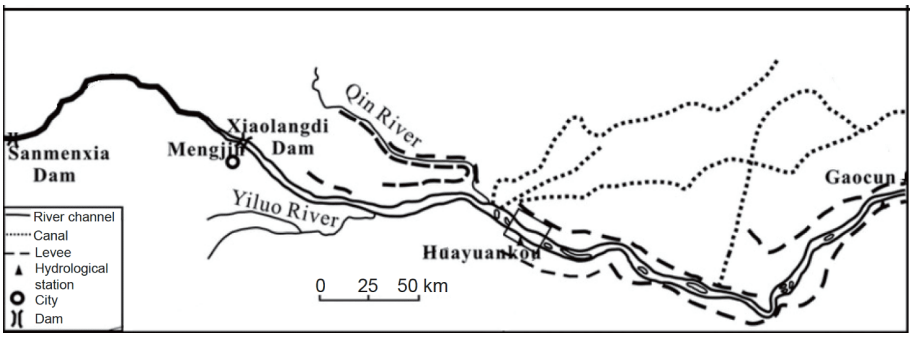

Figure 4 Locations of Xiaolangdi and Huanyoukou Gauge Stations along the Lower Yellow River.

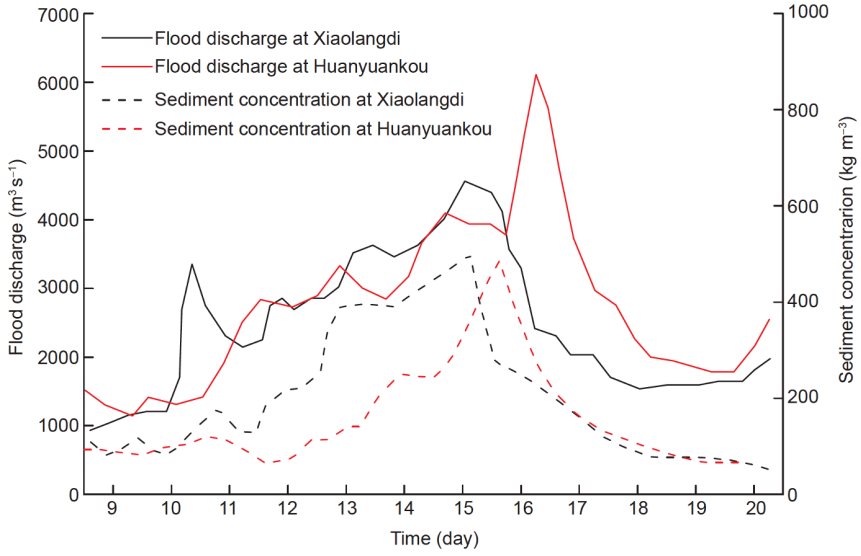

Figure 5 (Color online) Measured discharge and sediment concentration processes at Xiaolangdi and Huayuankou Gauge Stations [48].

two stages interacted during the propagation process, and the peak value of the flood peak reached 6260 $m^3 s^{-1}$ at the downstream Huayuankou Station. Amplification of downstream flood discharge is very different from common sense, but there was little rainfall or tributary confluence along the flood route. Figure 5 shows a uniform flow condition with equilibrium sediment transport. The flow discharge is 1000 $m^3 s^{-1}$, and the equilibrium sediment concentration s_{eq0} is 100 kg m^{-3}. Considering the average river width of 500 m in the reach between Xiaolangdi and Huayuankou, and the bankfull depth H_0 of about 10 m, the uniform flow velocity U_0 is calculated as 0.2 m s^{-1}.

Figure 6 shows a simulation of the flood route in the open channel between the Xiaolangdi and Huayoukou Gauge Stations in the "92.8" flood. The latter flood peak with a high propagation speed gradually "catches up" with the former that propagates slowly, resulting in the superposition of flow discharges. Moreover, the "92.8" flood developed into an almost single peak shape as it passed through Huayuankou Station. The peak flood discharge of Huayuankou Station reaches about 6000 $m^3 s^{-1}$, which is significantly higher than the flood discharge of 4500 $m^3 s^{-1}$ measured at the upstream Xiaolangdi Station. This can be explained by the characteristics of kinetic wave propagation in sediment-laden flows. Based on the analysis above, the kinetic wave propagation is affected by the equilibrium sediment concentration in a uniform flow. The higher the sediment concentration, the faster the kinetic wave propagates. The latter flood peak is significantly accelerated due to the rapid increase in sediment concentration, which is a key factor of the analytical solution obtained in this study. Figure 7 shows the temporal variation of flow discharge at Huayuankou Station. The calculated results are in good agreement with the measured data. The root mean square error is about 9.1%, and the overall accuracy is 90.9%. The phenomenon of increasing flow discharge is successfully simulated.

Figure 8 shows a comparison of simulation results and measured data of morphological evolution at Huayuankou Station. The "92.8" flood clearly shows that the riverbed has undergone rapid and extensive erosion and deposition. In the initial sections of the flood route, the flow intensity continues to increase, and the sediment capacity increases. Due to

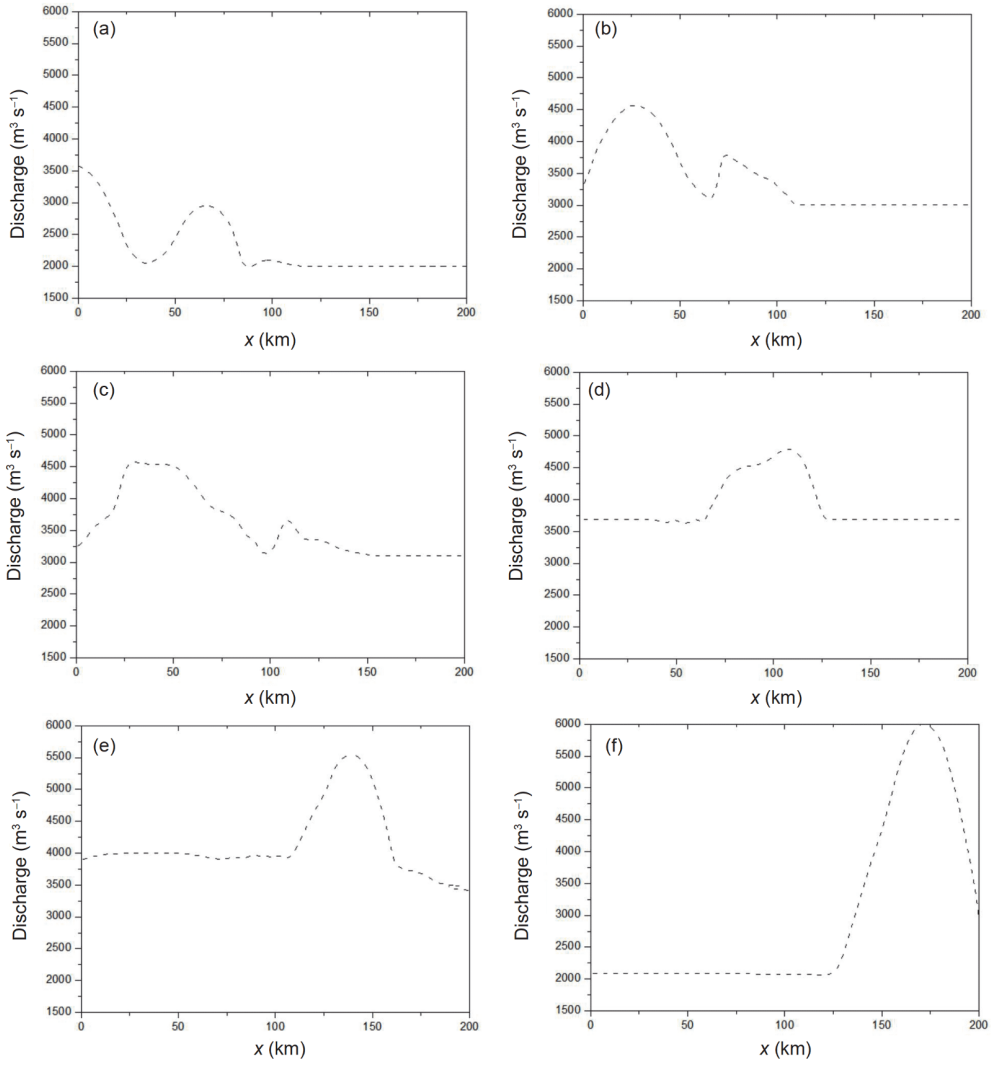

Figure 6 Simulation of flood route in the reach between Xiaolangdi and Huayuankou Stations. (a) t=80 h; (b) t=100 h; (c) t=120 h; (d) t=140 h; (e) t=160 h; (f) t=180 h.

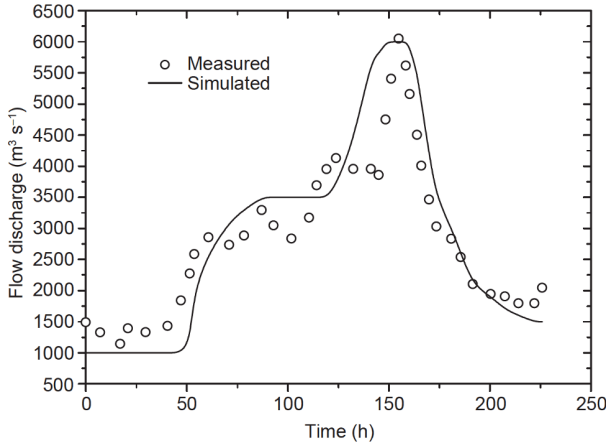

Figure 7 Simulated temporal variation of flow discharge at Huayuankou Station.

nonequilibrium sediment transport, the riverbed is gradually eroded. With the largest increase in flood peak, the elevation of the riverbed dropped to 4 m. Although sediments are hyperconcentrated in the floodwater, the morphological evolution is degraded. As the peak flood flow decreases, the flow intensity continues to weaken. Therefore, sediment concentrations become oversaturated due to former bed erosion, converting morphological evolution into deterioration. The root mean square error between simulation results and measured data of morphological evolution at Huayuankou Station is about 12.7%, and the overall accuracy is 87.3%. The calculation results shown in Figure 8 reasonably reflect the process of morphological evolution.

6 Concluding remarks

This study presents results on analytical solutions for 1D mathematical models of flow and morphological evolution in open channels. Complete governing equations that in-

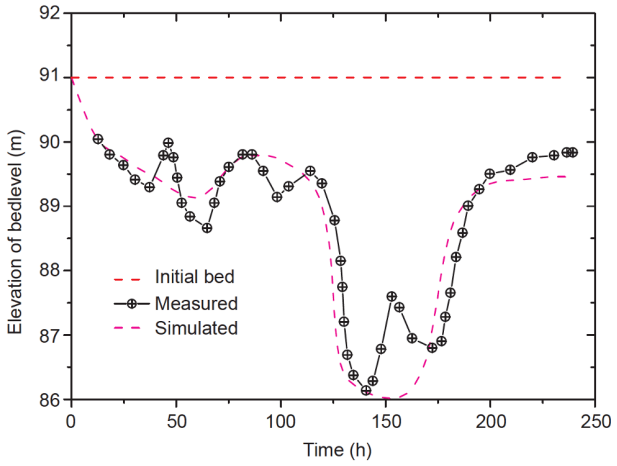

Figure 8 (Color online) Simulated temporal variation of bed level elevation at Huayuankou Station.

corporate the interaction of flow and sediment transport were adopted. In addition, singular perturbation and Laplace transform techniques were implemented.

A hierarchical equation of waves has been derived to explain the evolutionary nature of disturbances in hyperbolic systems. The wave hierarchy consists of three types of waves with different energy magnitudes: dynamic, diffusion, and kinetic waves. The propagation characteristics of these waves are different from each other. These three types of waves interact with each other during evolution. The dynamic wave depends only on the Froude number. Kinetic and diffusion waves are dependent on a coupling of sediment transport and river mobility. The higher the sediment concentration, the faster the kinetic wave propagation, but the slower the diffusion wave path.

An analytical solution was obtained by a linear combination of analytical expressions in the kinetic wave front and the diffusion wave front. The obtained analytical solution can describe the physical mechanism of motion in open channels as completely as possible. Analytical solutions are displayed as a combination of exponential functions, hyperbolic functions, and infinite series. The analytical solutions of eqs. (33) and (28) were applied by simulating the flood route with hyperconcentrated sediment transport in the Lower Yellow River region in China. It was found that the calculation results were in good agreement with the measured data. The phenomenon of increased flow discharge was successfully simulated, and the process of morphological evolution was reasonably explained.

The analytical solution derived in this study is based on the perturbation method with the following assumptions: (1) a relatively small perturbation, and (2) first-order perturbation. These assumptions can induce some discrepancies, as shown in Figures 7 and 8. However, local variations in the evolution of flow transport cannot be well represented. Mathematically, a set of governing equations for flow motion, sediment transport, and morphological evolution build a fourth-order nonlinear hyperbolic system. Strong nonlinearities often break the perturbed and asymptotic approximations of nonlinear problems. The homotopy analysis method can be adopted in future studies to improve the applicability of analytical solutions.

This work was supported by the National Key Research and Development Program of China (Grant No. 2016YFC0402503) and the National Natural Science Foundation of China (Grant No. 41876095). Valuable comments from the anonymous reviewers are highly appreciated, and help us considerably to improve the quality of this manuscript.

Supporting Information

The supporting information is available online at tech.scichina.com and link.springer.com. The supporting materials are published as submitted, without typesetting or editing. The responsibility for scientific accuracy and content remains entirely with the authors.

1 Ren M E, Shi Y L. Sediment discharge of the Yellow River (China) and its effect on the sedimentation of the Bohai and the Yellow Sea. Cont Shelf Res, 1986, 6: 785–810
2 Li J, Xie S P, Cook E R, et al. Deciphering human contributions to Yellow River flow reductions and downstream drying using centuries-long tree ring records. Geophys Res Lett, 2019, 46: 898–905
3 DHI Inc, 2003. 301 South State Street, Newtown, PA 18940, USA. http://www.dhisoftware.com/general/Contact_info.htm
4 US Army Corps Engineer. HEC-6: Scour and Deposition in Rivers and Reservoirs. User's Manual, 1993
5 Lai C. Numerical Modeling of Unsteady Open-Channel Flow. Adv Hydrosci, 1986, 14: 161–333
6 Zhou J, Lin B. One-dimensional mathematical model for suspended sediment by lateral integration. J Hydraul Eng, 1998, 124: 712–717
7 Cunge J A, Holly F M J, Verwey A. Practical Aspects of Computational River Hydraulics. London: Pitman Advanced Publishing Program, 1980
8 Lyn D A. Unsteady sediment transport modelling. J Hydraul Eng, 1987, 113: 1–15
9 Ni J R, Zhang H W, Xue A, et al. Modeling of hyperconcentrated sediment-laden floods in lower yellow river. J Hydraul Eng, 2004, 130: 1025–1032
10 Cui Y T, Paola C, Parker G. Numerical simulation of aggradation and downstream fining. J Hydraul Res, 1996, 34: 185–204
11 Wu W M. Computational River Dynamics. London: Taylor & Francis, 2007, doi: 10.4324/9780203938485
12 Ji C N, Ante M, Eldad A, et al. Numerical investigation of particle saltation in the bed-load regime. Sci China Tech Sci, 2014, 57: 1500–1511
13 Cao Z X, Day R, Egashira S. Coupled and uncoupled numerical modeling of flow and morphological evolution in alluvial rivers. J Hydraul Eng, 2002, 128: 306–321
14 Hu P, Cao Z X. Fully coupled mathematical modeling of turbidity currents over erodible bed. Adv Water Res, 2009, 32: 1–15
15 Cao Z X, Li Y, Yue Z Y. Multiple time scales of alluvial rivers carrying suspended sediment and their implications for mathematical modeling. Adv Water Res, 2007, 30: 715–729
16 Cao Z X, Hu P, Pender G. Multiple time scales of fluvial processes with bed load sediment and implication for mathematical modeling. J Hydraul Eng, 2011, 137: 267–276
17 Ding Y, Li Z S, Zhong D Y, et al. Coupling mechanism of mathematical models for sediment transport based on characteristic theory. Sci China Tech Sci, 2016, 59: 1696–1706

18 Ribberink J S, Van Der Sande J T M. Aggradation in rivers due to overloading: Analytical approaches. J Hydraul Res, 1985, 23: 273–283
19 Lyn D A, Altinakar M. St. Venant-Exner equations for near-critical and transcritical flows. J Hydraul Eng, 2002, 128: 579–587
20 Singh A K, Kothyari U C, Ranga Raju K G. Rapidly varying transient flows in alluvial rivers. J Hydraul Res, 2004, 42: 473–486
21 Li S S, Millar R G. Simulating bed-load transport in a complex gravel-bed river. J Hydraul Eng, 2007, 133: 323–328
22 Lisle T E, Cui Y, Parker G, et al. The dominance of dispersion in the evolution of bed material waves in gravel-bed rivers. Earth Surf Process Landforms, 2001, 26: 1409–1420
23 Kassem A A, Chaudhry M H. Comparison of coupled and semi-coupled numerical models for alluvial channels. J Hydraul Eng, 1998, 124: 794–802
24 Qian H L, Cao Z X, Pender G, et al. Well-balanced numerical modelling of non-uniform sediment transport in alluvial rivers. Int J Sediment Res, 2015, 30: 117–130
25 Ning J G, Wang X, Ma T B, et al. Numerical simulation of shock wave interaction with a deformable particle based on the pseudo arc-length method. Sci China Tech Sci, 2015, 58: 848–857
26 Zhu F, Dodd N. The morphodynamics of a swash event on an erodible beach. J Fluid Mech, 2015, 762: 110–140
27 Hamid M, Zubair T, Usman M, et al. Numerical investigation of fractional-order unsteady natural convective radiating flow of nanofluid in a vertical channel. AIMS Math, 2019, 4: 1416–1429
28 Hamid M, Usman M, Haq R U, et al. Wavelet analysis of stagnation point flow of non-Newtonian nanofluid. Appl Math Mech-Engl Ed, 2019, 40: 1211–1226
29 Zhu Y L, Luo J Q, Liu F. Flow computations of multi-stages by URANS and flux balanced mixing models. Sci China Tech Sci, 2018, 61: 1081–1091
30 Khan Z H, Khan W A, Tang J, et al. Entropy generation analysis of triple diffusive flow past a horizontal plate in porous medium. Chem Eng Sci, 2020, 228: 115980
31 Usman M, Hamid M, Khalid M S U, et al. A robust scheme based on novel-operational matrices for some classes of time-fractional nonlinear problems arising in mechanics and mathematical physics. Numer Methods Partial Differ Eq, 2020, 36: 1566–1600
32 Hamid M, Usman M, Haq R U, et al. A Chelyshkov polynomial based algorithm to analyze the transport dynamics and anomalous diffusion in fractional model. Physica A-Statistical Mech its Appl, 2020, 551: 124227
33 Marit J M, Muller E. The analytical solution of the Riemann problem in relativistic hydrodynamics. J Fluid Mech, 1994, 258: 317–333
34 Kazezyılmaz-Alhan C M, Medina Jr. M A. Kinematic and diffusion waves: Analytical and numerical solutions to overland and channel flow. J Hydraul Eng, 2006, 133: 217–228
35 Scholle M, Aksel N. An exact solution of visco-capillary flow in an inclined channel. Z Math Phys, 2001, 52: 749–769
36 Wu Z, Chen G Q. Analytical solution for scalar transport in open channel flow: Slow-decaying transient effect. J Hydrol, 2014, 519: 1974–1984
37 Desatnik M S, Qassim R Y. A new exact solution of one dimensional steady gradually varied flow in open channels. Eng Math, 2017, 1: 7–10
38 Risch P, Helmer D, Kotz F, et al. Analytical solution of the time-dependent microfluidic poiseuille flow in rectangular channel cross-sections and its numerical implementation in microsoft excel. Biosensors, 2019, 9: 67
39 Ponce V M, Li R N, Simons D B. Applicability of kinematic and diffusion models. J Hydraul Div Am Soc Civ Eng, 1978, 104: 353–360
40 Singh V P. Kinematic Wave Modeling in Water Resources-Surface Water Hydrology. New York: Wiley, 1996
41 Ferrick M G, Goodman N J. Analysis of linear and monoclinal river wave solutions. J Hydraul Eng, 1998, 124: 728–741
42 Tsai C W. Applicability of kinematic, noninertia, and quasi steady dynamic wave models to unsteady flow routing. J Hydraul Eng, 2003, 129: 613–627
43 Tayfur G, Singh V P. Kinematic wave model for transient bed profiles in alluvial channels under nonequilibrium conditions. Water Resour Res, 2007, 43: W12412
44 Barati R, Rahimi S, Akbari G H. Analysis of dynamic wave model for flood routing in natural rivers. Water Sci Eng, 2012, 5: 243–258
45 Huai W X, Yang L, Guo Y K. Analytical solution of suspended sediment concentration profile: Relevance of dispersive flow term in vegetated channels. Water Resour Res, 2020, 56: 6436–6449
46 Tsai C W S, Yen B C. Linear analysis of shallow water wave propagation in open channels. J Eng Mech, 2001, 127: 459–472
47 Hayami S. On the propagation of flood waves. Bulletin No. 1, Disaster Prevention Research Institute, Kyoto Univ. Kyoto, 1951: 1–6, http://hdl.handle.net/2433/123641
48 Tingsanchali T, Manandhar S K. Analytical diffusion model for flood routing. J Hydraul Eng, 1985, 111: 435–454
49 Zhang R J, Xie J H. Sedimentation Research in China: Systematic selections (in Chinese). Beijing: China Water Power Press, 1993
50 Needham D J. Wave hierarchies in alluvial river flows. Geophys Astrophys Fluid Dyn, 1990, 51: 167–194
51 Whitham G B. Linear and Nonlinear Waves. New York: John Wiley & Sons, Interscinece, 1974
52 Davis G B. A Laplace transform technique for the analytical solution of a diffusion-convection equation over a finite domain. Appl Math Model, 1985, 9: 69–71
53 Brown J W, Churchill R V. Complex Variables and Applications. New York: McGraw-Hill, 2009
54 Yellow River Conservancy Commission. Yellow River Yearbook (in Chinese). Ministry of Water Resources, Beijing, 1996